Appl Phys B (2009) 95: 281–286
DOI 10.1007/s00340-009-3423-1

Applied Physics B
Lasers and Optics

Infrared laser-spectroscopic analysis of ^{14}NO and ^{15}NO in human breath

K. Heinrich · T. Fritsch · P. Hering · M. Mürtz

Received: 16 October 2008 / Revised version: 28 January 2009 / Published online: 28 February 2009

Abstract We report on monitoring of nitric oxide (NO) traces in human breath via infrared cavity leak-out spectroscopy. Using a CO sideband laser near 5 μm wavelength and an optical cavity with two high-reflectivity mirrors ($R = 99.98\%$), the minimum detectable absorption is 2×10^{-10} cm^{-1} Hz$^{1/2}$. This allows for spectroscopic analysis of rare NO isotopologues with unprecedented sensitivity. Application to simultaneous online detection of ^{14}NO and ^{15}NO in breath samples collected in the nasal cavity is described for the first time. We achieved a noise-equivalent detection limit of 7 parts per trillion for nasal ^{15}NO (integration time: 70 s).

PACS 33.57.+c · 42.62.Fi

1 Introduction

The analysis of human breath for specific molecular trace gases is a promising diagnostic technique for investigating various health conditions. There is a particular interest in certain small molecular compounds such as NO, which has been identified as important messenger molecule in the human body. It is well known that NO is synthesized by a variety of biological tissues. It plays a major role in the regulation of blood pressure, in nerve cell communication, in the destruction of pathogens, and it is involved in numerous other physiological processes which currently are being investigated. In healthy subjects, the main sources for exhaled NO (eNO) are the upper airways, especially the nose and the nasopharynx [5].

Investigation of its importance and the roles it plays in the human body benefits from the ability to use and detect labeled NO, for example, the rare isotope ^{15}N (natural abundance: 0.365%) instead of the main isotope ^{14}N (99.4%). In particular, the use of ^{15}NO as an isotopic tracer from metabolized L-arginine, a precursor of NO, has been shown to be effective in monitoring certain physiological and pathophysiological processes [11, 21].

The specific and sensitive detection of NO isotopologues represents a continuing challenge in the field of NO research. Presently, the O_3/NO_2-chemiluminescence detection (CLD) method is the standard method to measure eNO concentrations in human breath [1, 24]. This method detects NO by its reaction with ozone to produce NO_2, O_2, and light, where the light is measured with a photomultiplier tube. However, CLD cannot discriminate between different NO isotopologues.

Laser absorption spectroscopy (LAS) provides a very powerful means for trace analysis with extremely high sensitivity, specificity, and speed. In particular, absorption spectroscopy in the mid-infrared region around 5 μm, where strong fundamental absorption bands for NO reside, is well suited for NO measurements. High-resolution LAS can distinguish between isotopologues based on the spectral shift of rotational-vibrational lines resulting from the different molecular mass. However, to detect ^{15}NO in natural abundance, an ultra-high sensitivity on the low parts-per-trillion (10^{-12}, ppt) level is required.

A number of approaches for the optical sensing of trace NO have been reported in the past. Mid-infrared laser spectrometers based on a multi-pass cell absorption platform achieve a typical NO detection limit on the order of one part per billion (10^{-9}, ppb) [8–10, 18, 21]. To achieve even better

K. Heinrich · T. Fritsch · P. Hering · M. Mürtz (✉)
Institut für Lasermedizin, Universität Düsseldorf, 40225 Düsseldorf, Germany
e-mail: muertz@uni-duesseldorf.de
Fax: +49-211-8113121

sensitivity, cavity-enhanced techniques are applied: either cavity ring-down spectroscopy (CRDS) or integrated cavity output spectroscopy (ICOS) which both use an optical cavity with high-reflectivity mirrors ($R > 99.9\%$) instead of a multi-pass cell to achieve a longer optical path length. Using CRDS with a LN_2 cooled cw quantum-cascade laser (QCL) near 5.2 μm, a noise-equivalent sensitivity at the sub-ppb level in several seconds was achieved with high-reflectivity mirrors ($R \sim 99.99\%$) [6]. With ICOS (also QCL-based), NO detection sensitivities on the low-ppb level were reported [7, 13, 19, 20]. More recently, McCurdy et al. reported an Off Axis-ICOS approach using a thermoelectrically cooled, pulsed, quantum-cascade laser, achieving a NO detection limit of 0.4 ppb within 1 s integration time [23]. However, none of these LAS approaches reached a sensitivity for NO in the low-ppt range.

In our laboratory, we use mid-infrared cavity leak-out spectroscopy (CALOS), a cw variant of CRDS, for ultrasensitive trace gas analysis of various biogenic molecules [17, 25]. CALOS enables NO measurements in the gas-phase with very high specificity and sensitivity. We reported time-resolved detection of ^{15}NO with a noise-equivalent concentration of 40 ppt (acquisition time: 1 s) [12]. Moreover, we carried out a cross-validation of our spectrometer with the CLD gold-standard method for NO analysis [24].

Here, we report on the performance of an improved CALOS system for the trace analysis of eNO isotopologues on the low-ppt level. The objective of the present work was the simultaneous analysis of ^{14}NO and ^{15}NO in human breath samples. We demonstrate the application of this spectrometer for the simultaneous detection of endogenous ^{14}NO and ^{15}NO in the nasal cavity.

2 Experimental

2.1 Laser spectrometer

The spectroscopic set-up is shown in Fig. 1. It mainly comprises a CO gas laser, a CdTe electro-optical modulator (EOM), a high-finesse ring-down cavity and a photodetector. The CO laser operates in a spectral range of 4.75 to 5.5 μm on more than 100 rovibrational $\Delta v = 1$ transitions with single-mode output powers up to 300 mW; the spectral line width is below 100 kHz (in 1 s). The laser frequency is stabilized on top of the gain profile via a standard $1f$ stabilization technique. The CO laser beam is sent to the EOM, operating at microwave frequencies, for the generation of tunable sidebands. These sidebands can be continuously tuned in a frequency range of 8 to 18 GHz above and below each CO laser line. The optical power of one sideband entering the ring-down cell is 10 to 40 μW for 100 mW of incident CO laser power. More details are described in [17].

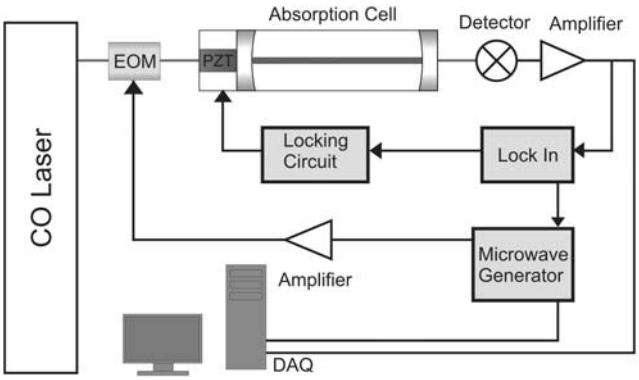

Fig. 1 Schematic of the CO-laser based spectroscopic set-up. The optical power of the tunable microwave sideband entering the absorption cell is near 100 μW. EOM: electro-optic modulator, PZT: piezoceramic transducer, DAQ: data acquisition

The laser beam is mode matched to the fundamental transverse mode of the ring-down cavity. The cavity mode is stabilized to the laser frequency, again by means of a standard $1f$ lock-in technique.

For this, the microwave frequency is modulated with a frequency of 600 Hz and an amplitude of 1.8 MHz. The transmitted signal through the cell is demodulated with a lock-in amplifier. After having passed through an integrator, the output of the lock-in amplifier is applied to a piezoelectric transducer, which holds one of the cavity mirrors.

The ring-down cell is home made and has been completely new designed. It basically consists of a glass tube held by an invar mount. Invar is a 36% nickel-iron alloy which has a very low thermal expansion coefficient (less than 1.7×10^{-6} K^{-1}) in the range from room temperature up to approximately 500 K and thus guarantees a high stability of the cavity length. The glass tube has a diameter of 18 mm and a length of 47 cm. At each end of the tube, a high-reflectivity plano-concave mirror (diameter = 20.3 mm, ROC = 6 m, $R = 99.98\%$ for $\lambda = 5$ μm) is held by an electric mount. These high-reflectivity mirrors increase the absorption path length up to several kilometers. The cell including the mirrors can be operated below ambient pressure. The mirror mounts are driven by electric set-and-hold vacuum actuators (Picomotor™, New Focus). They allow for fine tuning of the cavity mirrors with a step size of < 30 nm per step under low-pressure conditions. A free spectral range (FSR) of 276 MHz follows from a distance of 54.3 cm between the mirrors. The cell length was designed to exact this value in order that the frequency difference of the NO lines of interest is an integer multiple of the FSR (cf. Sect. 2.2). One mirror is mounted on a piezoelectric transducer to allow for fine tuning of the mirror distance.

For the trace gas measurements, the laser power is periodically injected into the ring-down cell, twice per modulation period. Each time the transmitted light indicates optimum coincidence of laser frequency and cavity mode, a

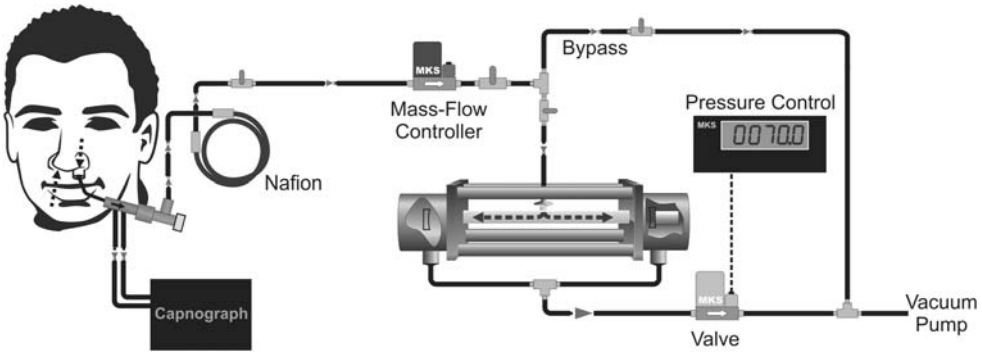

Fig. 2 Schematic of the breath sampling and gas system. The capnograph records the CO_2 concentration and the air flow rate in the nasal cavity. The breath sample is dried via a Nafion^{TM} tube before it enters the ring-down absorption cell. The gas flow through the cell is regulated with a mass-flow controller. Inside the cell the pressure is kept constant at 70 mbar

trigger pulse is provided to turn off the laser sideband radiation via the EOM. The subsequent leak-out of the light is monitored with a LN_2 cooled InSb photo detector (3.5 A/W at 1875 cm^{-1}), preamplified (10^5 V/A, 840 kHz bandwidth) and acquired by means of an analog-to-digital converter (50 MHz, 12 bit). The decay time ($1/e$ time) of each leak-out signal is determined by means of a fast exponential fitting algorithm [12] in real time and then averaged over 100 decays.

2.2 Breath sampling

Figure 2 shows the breath sampling set-up. This sampling was carried out according to the recommendations of the American Thoracic Society (ATS) and the European Respiratory Society (ERS), which have been published to standardize the technique of online and offline NO measurements in breath [16]. Following this, the measurement of nasal NO requires a transnasal air flow through the nostrils either in series or in parallel. To realize the flow in series, we transmitted room air from one nostril around the posterior nasal septum to the other nostril by means of a pump. In this way, air from the nasal cavity is collected and transmitted to the ring-down cell. We use a tight nose adapter and teflon tubing for reliable transmission of the gas sample. To remove water from the breath sample, the gas flow is dehumidified via a Nafion^{TM} tube. It was ensured that this does not affect the NO concentration. A mass-flow controller guarantees a constant flow through the cell, which is important to avoid pressure fluctuations inside the cell. A constant transnasal air flow rate after injecting the adapters into the nose generates a transient increase of NO followed by a constant plateau, which represents the steady-state NO concentration in the nasal cavity. A flow rate of 0.25 to 3 l/min is recommended, because this flow rate provides a steady plateau level of NO concentration in most subjects. Lower flow rates give higher NO concentrations. Here, we used air flow rates between 0.3 and 1.2 l/min. The pressure inside the ring-down cell is kept at 70 mbar. It should be noted that the NO level present in the room air was below our detection limit.

To avoid NO leakage from or to the nasal cavity, it is important to isolate the nasopharynx from the oral cavity and the airways. The ATS/ERS Recommendations list several possibilities to achieve closure of the velum. Here, a volunteer was trained to elevate the soft palate, which results in a closed velum. This closure can be verified by detecting the CO_2 concentration, which remains low (0.2%) when there is no air from the lower respiratory tract in the breath sample. We used a commercial capnograph (Datex Ohmeda) to continuously analyze both, the CO_2 level as well as the air flow through the nasal cavity.

3 Results and discussion

3.1 Detection limit

The signal-to-noise ratio of the observed absorption depends on the averaging time. In ideal cases, the precision of the mean value is proportional to the inverse square root of the averaging time. However, in the real world, there will be long-term drifts caused, e.g., by thermal effects, so that after a certain integration time longer averaging would not result in a better precision. The stability of the spectroscopic results can be analyzed using the Allan standard deviation $\sigma_\alpha(t)$, which was originally introduced to characterize the stability of oscillators and clocks [3].

The Allan variance is a two-sample variance defined as

$$\sigma_\alpha^2(t) = \frac{1}{2}\left\langle(\alpha_{n+1} - \alpha_n)^2\right\rangle,$$

where the brackets "$\langle\rangle$" denote a time averaging over t. To calculate the Allan deviation, the measured data are classified in n groups. α_n is the mean value of the values of the nth group, t is the time that is necessary to record the values of one group. The minimum of this deviation represents the optimal integration time to reach the best signal to noise ratio. To determine the detection limit of our system we recorded the ring-down time τ_0 of the empty cell for 500 s and calculated the Allan deviation from these data. In Fig. 3, the Allan deviation is plotted against the averaging time. It shows an optimal averaging time of 70 s corresponding to a noise-

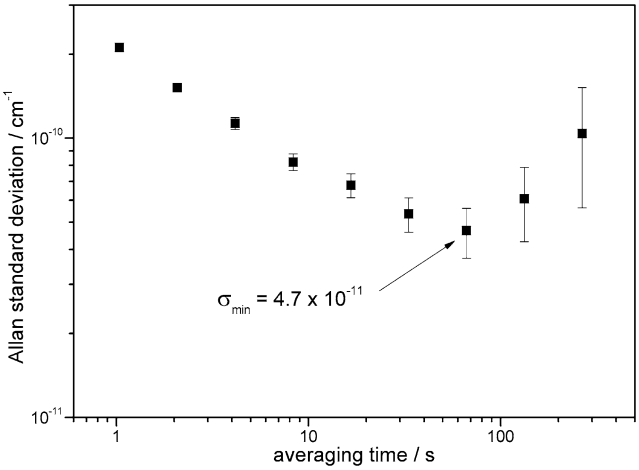

Fig. 3 Allan standard deviation of the observed absorption over averaging time. The optimum averaging time resulting in the minimum Allan deviation ($\sigma_{\min}$) is $t = 70$ s

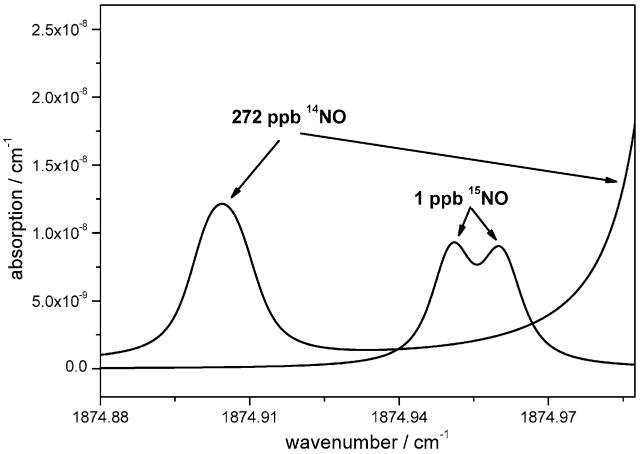

Fig. 4 Calculated spectrum of ^{14}NO and ^{15}NO in the spectral region near 1875 cm^{-1}. The spectra are based on the HITRAN2004 database and were calculated for the natural isotopic ratio. Temperature: 300 K. Pressure: 70 mbar

equivalent absorption of 4.7×10^{-11} cm^{-1}. For longer averaging times, drifts, e.g. thermal drifts, affect the precision of the absorption measurement. In comparison with the previous work of Halmer et al. [14], the optimum averaging time could be extended by a factor of 7, which indicates the considerably improved stability of the system.

The noise-equivalent absorption of 4.7×10^{-11} cm^{-1} corresponds to a noise-equivalent concentration of 6.6 ppt NO. This is sufficient for analysis of ^{15}NO originating from the upper airways. To our knowledge, this is the best detection limit for NO that has been achieved with a laser absorption spectrometer up to date. A slightly better sensitivity has been reported by Mitscherling et al. who developed a laser-induced fluorescence (LIF) technique for NO [22]. However, for isotopic tracing studies, it is essential to monitor not only the ^{15}NO level but to measure the ratio ^{15}NO/^{14}NO. A particular advantage of the infrared LAS approach is the capability to observe ^{14}NO and ^{15}NO simultaneously. We demonstrate the potential of our LAS set-up for simultaneous online measurements in the following section.

3.2 Simultaneous detection of ^{14}NO and ^{15}NO in breath

To demonstrate the spectrometer's capability for isotopic ratio measurements of biogenic NO in human breath, we studied the simultaneous analysis of ^{14}NO and ^{15}NO levels in the nasal cavity. The spectral region around 1874.9 cm^{-1} is appropriate to measure ^{14}NO and ^{15}NO, particularly to measure both simultaneously. This wavelength region is covered by the upper frequency sideband of the $P_9(9)$ CO laser line. An important advantage of this spectral windows is, that the absorption lines of both isotopologues exhibit comparable absorption when present in the natural ratio, which is $R_{\text{nat}} = [^{15}\text{NO}]/[^{14}\text{NO}] = 0.00365$. Figure 4 shows a calculated NO spectrum based on the HITRAN2004 database [15]; the concentrations are 1 ppb ^{15}NO and 272 ppb ^{14}NO, the pressure is 70 mbar. The spectrum exhibits two characteristic absorption lines of ^{15}NO and ^{14}NO with comparable absorption at natural isotope ratio. This is the Q(7.5), $^2\Pi_{1/2}$ transition of ^{14}NO at 1874.90 cm^{-1} and the R(9.5), $^2\Pi_{1/2}$ transition of ^{15}NO near 1874.95 cm^{-1}, which is splitted because of Λ doubling. Also, the relative strong absorption line at 1875.0 cm^{-1} corresponding to the Q(6.5), $^2\Pi_{3/2}$ transition of ^{14}NO, must be taken into account.

The output power of the $P_9(9)$ CO laser line is about 300 mW. By periodically switching the laser frequency between a ^{14}NO and ^{15}NO line (switching frequency: 3 Hz) we can measure both isotopologues almost at the same time. The cell length was designed in order that 5 times the FSR (5×276 MHz $= 1380$ MHz) exactly equals the frequency difference between the Q(7.5) transition of ^{14}NO at 1874.90 cm^{-1} and the R(9.5)e transition of ^{15}NO at 1874.95 cm^{-1} (which is the left peak of the Λ-doubled line). It takes about 150 ms to measure the ^{14}NO line and to change the laser frequency to the ^{15}NO line; each data point is the mean value of 100 consecutive ring-down time measurements. From the peak absorption values observed, the concentrations of ^{14}NO and ^{15}NO are determined using the line strengths given by the HITRAN2004 database. Since the ^{15}NO line is considerably overlapped by the Q(7.5) and Q(6.5) lines of ^{14}NO, the ^{15}NO line absorption was corrected by subtracting the corresponding absorption contribution from the ^{14}NO lines.

In the following we focus on the measurement of ^{14}NO and ^{15}NO in human breath. The volunteer was a male person (32 years old), non-smoker and had no history of respiratory diseases. Due to the finding that exhaled NO is increased after ingestion of nitrate-containing food, the volunteer refrained from eating 2 hours before the measurement. Before the measurement, the volunteer closed the velum and started

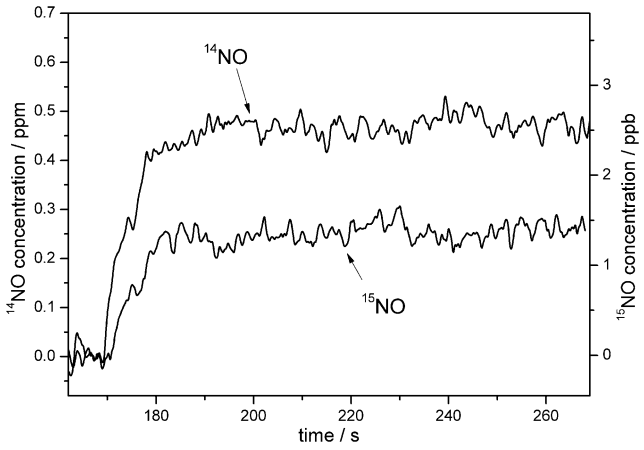

Fig. 5 Simultaneous online ^{14}NO and ^{15}NO measurement in the nasal cavity. The nose adapter was plugged into one nostril at $t = 170$ s. The transnasal air flow rate was 1.2 l/min, according to the recommendation of the ATS. The signals are smoothed by means of a running average over 1 s. Please note the different scales for ^{14}NO and ^{15}NO

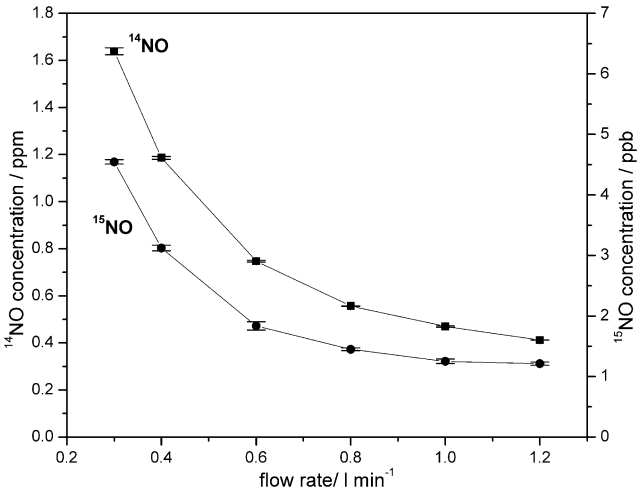

Fig. 6 Observed nasal ^{14}NO and ^{15}NO concentrations over the transnasal air flow rate. Each point is the time-averaged value over 70 s of NO concentration measurements. Please note the different scales for ^{14}NO and ^{15}NO

breathing through the mouth. He breathed in this way during the whole experiment. Then he introduced the nose adapter in one nostril. Now room air circulated around the septum into the detection cell.

Figure 5 shows the simultaneous measurement of ^{14}NO and ^{15}NO in this nasal gas sample. The transnasal air flow rate was 1.2 l/min, according to the recommendation of the ATS/ERS. After the volunteer applied the nose adapter, the NO concentration increased. After a transient phase of about 10 s, the concentration reached a steady-state plateau. It should be noted that the instrumental response time of the laser spectrometer is below 1 s.

The ^{14}NO concentration of the subject was determined from the data shown in Fig. 5 to be 470.45 ± 19.8 ppb (averaged over 70 s), and the ^{15}NO concentration was 1.38 ± 0.096 ppb (averaged over 70 s). The errors are the 1σ standard deviations of the mean values. From this, the isotope ratio can be calculated to be $R_{\text{sample}} = 0.00293 \pm 2.4 \times 10^{-4}$. The isotope ratio is often described by the value of $\delta^{15}\text{N} = [(R_{\text{sample}}/R_{\text{nat}}) - 1] \times 1000‰$. For the measurement shown in Fig. 5, we obtain $\delta^{15}N = -197 \pm 66‰$. This ratio considerably deviates from the expected natural value ($\delta^{15}N = 0$). This large deviation from the natural isotope ratio is unexpected. It cannot be explained by uncertainties of temperature or pressure of the gas sample. The systematic error by these effects can be calculated to be in the order of 1‰/K and 1‰/mbar, respectively. As already discussed in [14], the deviation is most likely attributed to incorrect values of the line strengths of ^{15}NO in the HITRAN2004 database. For comparison, we analyzed various synthetic gas mixtures consisting of 20 to 50 ppm NO in nitrogen and obtained $\delta^{15}N = -214.2 \pm 18‰$ in this case. This agrees within the 1σ standard deviations with the result from the breath sample reported above. This systematic error due to the line strength values leads to a constant offset of $\delta^{15}N$ and is of no importance for the precision. For example, for biomedical tracer application, changes in the isotope ratio have to be measured , i.e. the constant offset is irrelevant.

Finally, we studied the dependence of the steady-state nasal NO values from the transnasal air flow rate applied. Figure 6 shows the observed ^{14}NO and ^{15}NO concentration over the air flow rate through the nose. Each point is the time-averaged value over 70 s of NO concentration measurements. The error bars are the 1σ standard deviations of the mean values; they are almost too small to be visible. For low air flow the NO level increases up to 1.6 ppm ^{14}NO and 6 ppb ^{15}NO, respectively. The concentration of NO (denoted as [NO]) exhibited a hyperbolic relationship with the transnasal air flow rate ($\dot{V}_{\text{nasal}}$). This can be explained by a constant NO generation rate in the nasal cavity:

$$\text{net nitric output} = \dot{V}_{^{14}\text{NO}} = [^{14}\text{NO}] \times \dot{V}_{\text{nasal}} = \text{const.}$$

The average nasal NO output $\dot{V}_{^{14}\text{NO}}$ of the measurements displayed in Fig. 6 is 471 ± 21 nl/min. This value is within the expected physiological range and in agreement with previous reports [2, 4].

4 Conclusion

We reported a CALOS spectrometer optimized for ^{15}NO/^{14}NO online measurements in nasal air. The development of a 50-cm-long high-finesse optical cavity with improved mechanical and thermal stability resulted in a detection limit for NO in the low-ppt range. Due to the distinguishable absorption spectra of different isotopologues, CALOS is able

to differentiate between ^{14}NO and ^{15}NO; this is of great interest for biomedical research studies, e.g. to distinguish between endogenous and exogenous sources by using labeled NO and NO derivatives. The excellent time resolution (<1 s) allowed us to detect ^{14}NO and ^{15}NO simultaneously. As an application we presented an online measurement of ^{14}NO and ^{15}NO in nasal air. The precision of the $^{15}NO/^{14}NO$ ratio measurement is sufficient for tracer studies if the relative change in ^{15}NO exceeds 5%. Additional improvement in sensitivity and precision can be obtained by using a more powerful laser source (>1 mW). The described spectrometer is bound to the laboratory. A mobile set-up would be based on a QCL, which may replace the CO laser. Work along these lines is in progress in our laboratory.

Acknowledgements This work is part of the Ph.D. thesis of Kathrin Heinrich at the faculty of mathematics and science at the Heinrich-Heine-Universität Düsseldorf. We acknowledge financial support by the Deutsche Forschungsgemeinschaft.

References

1. L.E. Gustafsson, A.M. Leone, M.G. Persson, N.P. Wiklund, S. Moncada, Endogenous nitric oxide is present in the exhaled air of rabbits, guinea pigs and humans. Biochem. Biophys. Res. Commun. **181**, 852–857 (1991)
2. M. Imada, J. Iwamoto, S. Nonaka, Y. Kobayashi, T. Unno, Measurement of nitric oxide in human nasal airway. Eur. Respir. J. **9**, 556–559 (1996)
3. D.W. Allan, N. Ashby, C.C. Hodge, The science of timekeeping. Hewlett Packard Appl. Note **1289**, 56–71 (1997)
4. P.G. Djupesland, J.M. Chatkin, W. Qian, P. Cole, N. Zamel, P. Mcclean, H. Furlott, J.S.J. Haight, Aerodynamics influences on nasal nitric oxide output measurements. Acta Oto-Laryngol. **119**, 479–485 (1999)
5. S.A. Kharitonov, P.J. Barnes, Exhaled markers of pulmonary disease. Am. J. Respir. Crit. Care Med. **163**, 1693–1722 (2001)
6. A.A. Kosterev, A.L. Malinovsky, F.K. Tittel, C. Gmachl, F. Capasso, D.L. Sivco, J.N. Baillargeon, A.L. Hutchinson, A.Y. Cho, Cavity ring down spectroscopic detection of nitric oxide with a continuous-wave quantum-cascade laser. Appl. Opt. **40**, 5522–5529 (2001)
7. L. Menzel, A.A. Kosterev, R.F. Curl, F.K. Tittel, C. Gmachl, F. Capasso, D.L. Sivco, J.N. Baillargeon, A.L. Hutchinson, A.Y. Cho, W. Urban, Spectroscopic detection of biological NO with a quantum cascade laser. Appl. Phys. B **72**, 859–863 (2001)
8. C. Roller, K. Namjou, J.D. Jeffers, M. Camp, A. Mock, P.J. McCann, J. Grego, Nitric oxide breath testing by tunable-diode laser absorption spectroscopy: application in monitoring respiratory inflammation. Appl. Opt. **41**, 6018–6029 (2002)
9. D.D. Nelson, J.H. Shorter, J.B. McManus, M.S. Zahniser, Sub-part-per-billion detection of nitric oxide in air using a thermoelectrically cooled mid-infrared quantum cascade laser spectrometer. Appl. Phys. B **75**, 343–350 (2002)
10. W.H. Weber, T.J. Remillard, R.E. Chase, J.F. Richert, F. Capasso, C. Gmachl, A.L. Hutchinson, D.L. Sivco, J.N. Baillargeon, A.Y. Cho, Using a wavelength-modulation quantum cascade laser to measure *NO* concentration in the parts-per-billion range for vehicle emissions certification. Appl. Spectrosc. **56**, 706–714 (2002)
11. Y.C. Luiking, N.E. Deutz, Isotopic investigation of nitric oxide metabolism in disease. Curr. Opin. Clin. Nutr. Metab. Care **6**, 103–108 (2003)
12. D. Halmer, G. von Basum, P. Hering, M. Mürtz, Fast exponential fitting algorithm for real-time instrumental use. Rev. Sci. Instrum. **75**, 2187–2191 (2004)
13. M.L. Silva, D.M. Sonnenfroh, D.I. Rosen, M.G. Allen, A. O' Keefe, Integrated cavity output spectroscopy measurements of NO levels in breath with a pulsed room-temperature QCL. Appl. Phys. B **81**, 705–710 (2005)
14. D. Halmer, G.V. Basum, M. Horstjann, P. Hering, M. Mürtz, Time resolved simultaneous detection of ^{14}NO and ^{15}NO via mid-infrared cavity leak-out spectroscopy. Isot. Environ. Health Stud. **41**, 303–311 (2005)
15. L.S. Rothman, D. Jacquemart, D.C. Barbe, D.C. Benner, M. Birk, L.R. Brown, M.R. Carleer, C. Chackerian, K. Chance, L.H. Coudert, V. Dana, V.M. Devi, J.M. Flaud, R.R. Gamache, A. Goldman, J.M. Hartmann, K.W. Jucks, A.G. Maki, J.Y. Mandin, S.T. Massie, J. Orphal, A. Perrin, C.P. Rinsland, M.A.H. Smith, J. Tennyson, R.N. Tolchenov, R.A. Toth, J. Vander Auwera, P. Varanasi, G. Wagner, The HITRAN 2004 molecular spectroscopic database. J. Quant. Spectrosc. Radiat. Transf. **96**, 139–204 (2005)
16. American Thoracic Society (ATS), the European Respiratory Society (ERS), ATS/ERS recommendations for standardized procedures for the online and offline measurement of exhaled lower respiratory nitric oxide and nasal nitric oxide, 2005. Am. J. Respir. Crit. Care Med. **171**, 912–930 (2005)
17. M. Mürtz, D. Halmer, M. Horstjann, S. Thelen, P. Hering, Ultra sensitive trace gas detection for biomedical applications. Spectrochim. Acta, Part A, Mol. Biomol. Spectrosc. **63**, 963–969 (2006)
18. B.W.M. Moeskops, S.M. Cristescu, F.J.M. Harren, Sub-part-per-billion monitoring of nitric oxide by use of wavelength modulation spectroscopy in combination with a thermoelectrically cooled, continuous-wave quantum cascade laser. Opt. Lett. **31**, 823–825 (2006)
19. Y.A. Bakhirkin, A.A. Kosterev, R.F. Curl, F.K. Tittel, D.A. Yarekha, L. Hvozdara, M. Giovannini, J. Faist, Sub-ppbv nitric oxide concentration measurements using cw thermoelectrically cooled quantum cascade laser-based integrated cavity output spectroscopy. Appl. Phys. B **82**, 149–154 (2006)
20. M.R. McCurdy, Y.A. Bakhirkin, F.K. Tittel, Quantum cascade laser-based integrated cavity output spectroscopy of exhaled nitric oxide. Appl. Phys. B **85**, 445–452 (2006)
21. J. Yi, K. Namjou, Z.N. Zahran, P.J. McCann, G.B. Richter-Addo, Specific detection of gaseous NO and ^{15}NO in the headspace from liquid-phase reactions involving NO-generating organic, inorganic, and biochemical samples using a mid-infrared laser. Nitric Oxide **15**, 154–162 (2006)
22. C. Mitscherling, J. Lauenstein, C. Maul, A.A. Veselov, O.S. Vasyutinskii, K.H. Gericke, Non-invasive and isotope-selective laser-induced fluorescence spectroscopy of nitric oxide in exhaled air. J. Breath Res. **1**, 026003 (2007)
23. M.R. McCurdy, Y. Bakhirkin, G. Wysocki, F.K. Tittel, Performance of an exhaled nitric oxide and carbon dioxide sensor using quantum cascade laser-based integrated cavity output spectroscopy. J. Biomed. Optics **12**, 034034 (2007)
24. T. Fritsch, P. Brouzos, K. Heinrich, M. Kelm, T. Rassaf, P. Hering, P. Kleinbongard, M. Mürtz, NO detection in biological samples: differentiation of ^{14}NO and ^{15}NO using infrared laser spectroscopy. Nitric Oxide **19**, 50–56 (2008)
25. T. Fritsch, M. van Herpen, G. von Basum, P. Hering, M. Mürtz, Is exhaled carbon monoxide level associated with blood glucose level? A comparison of two breath analyzing methods. J. Biomed. Opt. **13**, 034012 (2008)